

Diversity Enhancement via Magnitude

Steve Huntsman

Abstract—Promoting and maintaining diversity of candidate solutions is a key requirement of evolutionary algorithms in general and multi-objective evolutionary algorithms in particular. In this paper, we use the recently developed theory of *magnitude* to construct a gradient flow and similar notions that systematically manipulate finite subsets of Euclidean space to enhance their diversity, and apply the ideas in service of multi-objective evolutionary algorithms. We demonstrate diversity enhancement on benchmark problems using leading algorithms, and discuss extensions of the framework.

Index Terms—magnitude, diversity, multiobjective evolutionary algorithm

I. INTRODUCTION

Promoting and maintaining diversity of candidate solutions is a key requirement of *evolutionary algorithms* (EAs) in general and *multi-objective EAs* (MOEAs) in particular [1], [2]. Many ways of measuring diversity have been considered, and many shortcomings identified [3]. Perhaps the most theoretically attractive diversity measure, used by [4], [5], is the *Solow-Polasky diversity* [6]. It turns out that a recently systematized theory of diversity in generalized metric spaces [7] singles out the Solow-Polasky diversity or *magnitude* of a (certain frequently total subset of a) finite metric space as equal to the maximum value of the “correct” definition (1) of diversity that uniquely satisfies various natural desiderata.¹ While the notion of magnitude was introduced in the mathematical ecology literature over 25 years ago, an underlying notion of a diversity-maximizing probability distribution is much more recent and to our knowledge has not yet been applied to EAs.

In the context of MOEAs, a practical shortcoming associated with magnitude is the typical $O(n^3)$ cost of matrix inversion. To avoid this, [4], [5] resort to a heuristic approximation for the sake of efficiency and merely *measure* diversity rather than attempting to *enhance* it from first principles.

However, it is profitable to incur the marginal cost of computing a so-called weighting *en route* to the magnitude, since we can use a weighting to enhance diversity near the boundary of the image of the candidate solution set under the objective functions. The nondominated part of this image is the current approximation to the Pareto front, and the ability of weightings to couple both diversity and convergence to the Pareto front dovetails with recent indicator-based EA approaches to Pareto-dominance based MOEAs [8], [9].² Moreover, the agnosticism of weightings to dimension further enhances their suitability for such applications.

S. Huntsman is with Systems and Technology Research, Arlington, VA, 22203 USA e-mail: steve.huntsman@str.us.

Manuscript received January 1, 1970; revised January 19, 2038.

¹In fact, [6] is the initial appearance of the magnitude concept.

²NB. Common performance indicators induce high density on the boundary of and singularities of the Pareto front [9]. We expect weightings to avoid at least the first of these concentration phenomena.

In this paper, we construct a gradient flow and similar mechanisms that systematically manipulate finite subsets of Euclidean space to enhance their diversity, which provides a useful primitive for quality diversity [10]. We then apply these ideas in service of multi-objective evolutionary algorithms by diversifying solution data through local mutations. For the sake of illustration, we only perform these mutations on the results of a MOEA, though they generally can and should be performed during the course of evolution.

The paper is organized as follows. In §II, we introduce the basic concepts of weightings, magnitude, and diversity. In §III, we identify an efficiently computable “positive cutoff” scale above which a weighting is guaranteed to be proportional to the unique diversity-maximizing distribution. In §IV, we develop a notion of a weighting gradient (estimate) and an associated gradient flow. In §V, we use this gradient flow to demonstrate diversity enhancement on a toy problem before turning to benchmark problems in §VI. Finally, we discuss algorithmic extensions and discrete analogues in §VII and §VIII, respectively, before making brief remarks in §IX. Appendix §A discusses an “erosion” procedure that is relevant to culling a population.

II. WEIGHTINGS, MAGNITUDE, AND DIVERSITY

For details on the ideas in this section, see §6 of [7].

Call a square nonnegative matrix Z a *similarity matrix* if its diagonal is strictly positive. An important class of similarity matrices is of the form $Z = \exp[-td]$ where the exponential is componentwise,³ $t \in (0, \infty)$, and d is a square matrix whose entries are in $[0, \infty]$ and satisfy the triangle inequality. In this paper, d will always be the matrix of distances for a finite subset of Euclidean space unless otherwise specified.

A *weighting* w is a column vector satisfying $Zw = 1$, where the vector of all ones is indicated on the right.⁴ A *coweighting* is the transpose of a weighting for Z^T . If Z admits both a weighting w and a coweighting, then its *magnitude* is defined via $\text{Mag}(Z) := \sum_j w_j$, which also turns out to equal the sum of the coweighting components.

In the case $Z = \exp[-td]$ and d is the distance matrix corresponding to a finite subset of Euclidean space, Z is

³For a matrix M and well behaved function f , we follow a standard practice in writing $(f[M])_{jk} := f(M_{jk})$ to distinguish a function applied to matrix entries versus to the matrix itself in the sense of functional calculus. Thus, e.g., $\exp[M] \neq \exp(M) = I + M + M^2/2! + \dots$.

⁴In Euclidean space, $Z = \exp[-td]$ is a radial basis function interpolation matrix [11] and the weighting equation $Zw = 1$ amounts to the statement that the weighting w provides the coefficients for interpolating the unit function. That is, if $\{x_j\}_{j=1}^n$ are points in Euclidean space with distance matrix d and we have a weighting w satisfying $\sum_k w_k \exp(-td_{jk}) = 1$, then in fact $u(x) := \sum_k w_k \exp(-t|x - x_k|) \approx 1$, where \approx indicates an optimal interpolation in the sense of a representer theorem [12]. In particular, the triangle inequality yields $u(x_j + \delta x_j) \geq \exp(-t|\delta x_j|)$.

positive definite, hence invertible, and so its weighting and magnitude are well-defined and unique.⁵ More generally, if Z is invertible then $\text{Mag}(Z) = \sum_{j,k} (Z^{-1})_{jk}$. For a generalized metric space d of the form specified above, the *magnitude function* $\text{Mag}(t; d)$ is defined as the map $t \mapsto \text{Mag}(\exp[-td])$.

It turns out [14], [15] that weightings are excellent scale-dependent boundary detectors in Euclidean space (see, e.g., Figure 2). In particular, if A is compact and $B \subset A$ is reasonably nice and finite (e.g., a uniform random sample or intersection with a regular lattice), then the largest components of a weighting on B tend to occur near the boundary of A . Meanwhile, any negative weighting components (if they exist) tend to be “just behind the boundary” of A (see §A). A technical explanation for this boundary-detecting behavior draws on the potential-theoretical notion of Bessel capacities [16].⁶ Our own investigations of asymmetric and thus manifestly non-Euclidean distances suggest that (co)weightings also indicate the presence of boundary-like features in those settings.

Meanwhile, magnitude is a very attractive and general notion of size that encompasses both cardinality and Euler characteristic, as well as encoding other rich scale-dependent geometrical data [19].

Example 1. Consider $\{x_j\}_{j=1}^3 \subset \mathbb{R}^2$ with pairwise distances $d_{jk} := d(x_j, x_k)$ given by $d_{12} = d_{13} = 1 = d_{21} = d_{31}$ and $d_{23} = \delta = d_{32}$ with $\delta < 2$. A routine calculation yields that

$$w_1 = \frac{e^{(\delta+2)t} - 2e^{(\delta+1)t} + e^{2t}}{e^{(\delta+2)t} - 2e^{\delta t} + e^{2t}}$$

and

$$w_2 = w_3 = \frac{e^{(\delta+2)t} - e^{(\delta+1)t}}{e^{(\delta+2)t} - 2e^{\delta t} + e^{2t}}.$$

This is shown in Figure 1 for $\delta = 10^{-3}$. At $t = 10^{-2}$, the “effective size” of the nearby points is ≈ 0.25 , and that of the distal point is ≈ 0.5 , so the “effective number of points” at this scale is ≈ 1 . At $t = 10$, these effective sizes are respectively ≈ 0.5 and ≈ 1 , so the effective number of points is ≈ 2 . Finally, at $t = 10^4$, the effective sizes are all ≈ 1 , so the effective number of points is ≈ 3 .

The notion of magnitude has been used by ecologists to quantify diversity since the work of Solow and Polasky [6], but much more recent mathematical developments have clarified the role that magnitude and weightings play in maximizing a more general and axiomatically supported notion of diversity

⁵ In Euclidean space, $Z = \exp[-td]$ is just a Laplacian kernel, which is positive definite [13].

⁶ For the case of an interval in \mathbb{R} this has been examined in detail: see the discussion following Proposition 5.9 of [16]. More generally, the weighting of compact $A \subset \mathbb{R}^n$ (defined for infinite A via a suitable technical procedure) is the distribution $\frac{1}{n! \omega_n} (I - \Delta)^{(n+1)/2} h$, where ω_n is the volume of the unit ball in \mathbb{R}^n and h is the Bessel potential function of A . The Bessel potential function is defined in turn as the function that takes the value 1 on A and minimizes the Bessel potential space norm, which generalizes the notion of a Sobolev norm. Another less precise but more computationally expedient manifestation of the same idea arises from an identity of Varadhan [17] that is equivalent to $(I - [\frac{n+1}{t}]^2 \Delta)^{-(n+1)/2} = \exp(-td + o(t^{-1}))$ for manifolds. Using a fast algorithm for the Laplacian can be computationally favorable, as discussed in Remark 4.19 of [18].

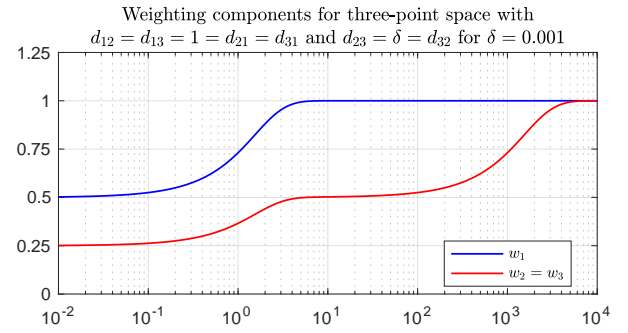


Fig. 1. Weighting components for an “isocoles” metric space. The magnitude function $w_1 + w_2 + w_3$ gives a scale-dependent “effective number of points.”

[7], [20]. Specifically, the *diversity of order q* for a probability distribution p and similarity matrix Z is the exponent of

$$\frac{1}{1-q} \log \sum_{j:p_j > 0} p_j (Zp)_j^{q-1} \quad (1)$$

for $1 < q < \infty$, and via limits for $q = 1, \infty$.⁷ This is the “correct” measure of diversity in essentially the same way that Shannon entropy is the “correct” measure of information. With this in mind, we restrict our attention to it versus other measures such as those discussed in [2], [3].

If Z is symmetric, then the (unique) positive weighting of the submatrix on common row and column indices that has the largest magnitude is proportional to the diversity-saturating distribution for *all* values of the free parameter q in the definition, and this magnitude equals the maximum diversity. In general the diversity-maximizing distribution is NP-hard to compute, though cases of size ≤ 25 are easily handled on a laptop. Fortunately, the situation improves radically if besides being symmetric, Z is also positive definite (as guaranteed for the metric on finite subsets of Euclidean space) and admits a positive weighting. Then this (unique) weighting is proportional to the diversity-maximizing distribution, and standard linear algebra suffices to obtain it efficiently.

Using an efficiently computable “diagonal cutoff” scale factor $t = t_d$ defined in Lemma 1, we can optimally enforce this advantageous situation for similarity matrices of the form $Z = \exp[-td]$. With t_d in hand, we can also efficiently identify a “positive cutoff,” i.e., the smallest scale $t_+ \leq t_d$ at which the weighting is automatically guaranteed to be proportional to a diversity-maximizing distribution.

This in turn allows us to define a gradient flow that increases the diversity of finite subsets of Euclidean space. This gradient flow is a principled and computationally efficient primitive for diversity optimization that informs evolutionary algorithms in Euclidean spaces. More generally, this gradient flow can also be defined on “positive definite metric spaces” [21] with vector space structure. Stochastic mechanisms that increase diversity on essentially arbitrary spaces satisfying a triangle inequality can be constructed as in §VIII.

⁷The expression (1) is a “similarity-sensitive” generalization of the Rényi entropy of order q . In the event $Z = I$, the usual Rényi entropy is recovered, with Shannon entropy as the case $q = 1$.

III. CUTOFF AND ZERO SCALES

In this section, we introduce two relevant scale factors associated with finite metric spaces, most notably a “positive cutoff” t_+ that is the minimal scale factor above which a weighting is proportional to a diversity-maximizing distribution. Besides allowing us to efficiently link weightings and diversity, using this scale factor also allows us to eliminate an unwanted degree of freedom in the definition of a weighting. For completeness, we also outline the behavior of scale factors approaching infinity and zero.

For similarity matrices that are ultrametric⁸ or diagonally dominant⁹ and of the form $\exp[-d]$ with d symmetric, non-negative, and with zero diagonal, there is a polynomial-time algorithm to compute the diversity-maximizing distribution that is also practical and admits ample scope for acceleration. This algorithm is just to normalize the weighting.

For d with zero diagonal and all other entries positive, there exists a minimal $t_d > 0$ such that $\exp[-td]$ is diagonally dominant for any $t > t_d$. We call t_d the *diagonal cutoff*. Because $\exp[-td]$ is diagonally dominant iff $1 > \max_j \sum_{k \neq j} \exp(-td_{jk})$, we can efficiently estimate t_d to any desired precision using the following elementary bounds and a binary search:

Lemma 1. For $d \in M_n$ as above,¹⁰

$$\frac{\log(n-1)}{\min_j \max_k d_{jk}} \leq t_d \leq \frac{\log(n-1)}{\min_j \min_{k \neq j} d_{jk}}. \quad (2)$$

Proof. If $\exp[-td]$ is diagonally dominant, then

$$\begin{aligned} 1 &> (n-1) \cdot \max_j \min_{k \neq j} \exp(-td_{jk}) \\ \iff 1 &> (n-1) \cdot \exp\left(-t \cdot \min_j \max_{k \neq j} d_{jk}\right) \\ \iff \log(n-1) &< t \cdot \min_j \max_k d_{jk}, \end{aligned}$$

which yields the first inequality in (2). Meanwhile, $\exp[-td]$ is diagonally dominant if

$$\begin{aligned} 1 &> (n-1) \cdot \max_j \max_{k \neq j} \exp(-td_{jk}) \\ \iff 1 &> (n-1) \cdot \exp\left(-t \cdot \min_j \min_{k \neq j} d_{jk}\right) \\ \iff \log(n-1) &< t \cdot \min_j \min_{k \neq j} d_{jk}, \end{aligned}$$

which yields the second inequality in (2). \square

⁸The ultrametric triangle inequality is $d(x, z) \leq \max\{d(x, y), d(y, z)\}$. Given a nonnegative symmetric matrix with zero diagonal, we can construct the unique maximal subdominant ultrametric (viz., the maximal hop in a minimal-weight path) using a spanning tree construction as in §IV.C of [22].

⁹Recall that a square matrix over \mathbb{R} is diagonally dominant if each diagonal element exceeds the sum of the other entries in its row.

¹⁰A metric d on $\{1, \dots, n\}$ is called *scattered* if $d(x, y) > \log(n-1)$ for all $x \neq y$ (see, e.g., Definition 2.12 of [23]). A corollary of Lemma 1 that amounts to Proposition 2.4.17 of [23] is that the diagonal cutoff of a scattered metric space is strictly less than 1.

As foreshadowed, we can also use Lemma 1 to find the *positive cutoff*, defined as the smallest $t_+ < t_d$ such that $\exp[-td]$ admits a positive weighting for $t > t_+$.¹¹

The limit $t \uparrow \infty$ of (co)weightings and the magnitude function is uninteresting: the (co)weightings are (co)vectors of all ones, and the limiting value of the magnitude function is thus just the number of points in the space under consideration. However, as Figure 2 suggests, the limit $t \downarrow 0$ contains more detailed structural information. The functional form of this limit is not hard to obtain:

Lemma 2. For $d \in GL(n, \mathbb{R})$ the solution to $\exp[-td]w(t) = 1$ (where as usual the exponential is elementwise) has the well-defined limit $w(0) := \lim_{t \downarrow 0} w(t) = \frac{d^{-1}1}{1^T d^{-1}1}$. Similarly, the solution to $v(t) \exp[-td] = 1$ has the limit $v(0) = \frac{1^T d^{-1}}{1^T d^{-1}1}$.¹²

Proof (sketch). We have the first-order approximation $(11^T - td)w(t) \approx 1$. Applying the Sherman-Morrison-Woodbury formula [24] and L’Hôpital’s rule yields the result. \square

IV. THE WEIGHTING GRADIENT FLOW

Although there are various sophisticated approaches to estimating gradients on point clouds (see, e.g., [25]), a reasonable heuristic estimate for the specific case of the gradient of a weighting w on $\{x_j\}_j$ in Euclidean space is

$$(\hat{\nabla} w)_j := \sum_{k \neq j} \frac{Z_{jk}}{\sum_{k' \neq j} Z_{jk'}} \frac{w_k - w_j}{d_{jk}} e_{jk} \quad (3)$$

where $e_{jk} := \frac{x_k - x_j}{d_{jk}}$.

Example 2. Figure 2 illustrates how weightings identify boundaries at various scales; Figure 3 shows the corresponding weighting gradient estimates (3).

It might appear that the *weighting gradient flow*

$$\dot{x} = \hat{\nabla} w \quad (4)$$

induced by (3) merely drives points apart, but Example 3 shows that the phenomenology is more nuanced.^{13 14}

Example 3. Continuing Example 1, assume without loss of generality that $(x_1)_2 = 0 = (x_2)_2 + (x_3)_2$. Now

$$(\hat{\nabla} w)_1 = \frac{\sqrt{4 - \delta^2}}{2} \frac{e^{(\delta+1)t} - e^{2t}}{e^{(\delta+2)t} - 2e^{\delta t} + e^{2t}} e_1$$

and

$$(\hat{\nabla} w)_2 = \frac{e^{-t}}{e^{-t} + e^{-\delta t}} \frac{e^{2t} - e^{(\delta+1)t}}{e^{(\delta+2)t} - 2e^{\delta t} + e^{2t}} e_{21}.$$

¹¹Outside the Euclidean setting, it makes sense to define t_+ to be the minimal value of t such that $Z = \exp[-td]$ admits a positive weighting and Z is positive semidefinite for $t > t_+$. But in the Euclidean setting, we get positive definiteness for free: see footnote 5.

¹²It would be interesting and probably also useful to characterize the quality of the approximation $w(t) \approx 1 + e^{-t} \frac{(d^{-1}1 - 1)}{1^T d^{-1}1}$. More generally, the same could be said of the approximation $I + e^{-t} \frac{(d^{-1}1 - I)}{1^T d^{-1}1} \approx Z^{-1}$. Probably a decent answer should inform (or be informed by) results on Bessel potentials and/or the Varadhan identity (see footnote 6).

¹³Although the weighting gradient flow (4) is for our purposes a finite system of coupled nonlinear ODEs, it seems likely in light of footnote 6 that this is an analogue of some extrinsic geometric flow in the sense of [26].

¹⁴Nevertheless, it seems likely that the weighting gradient flow (4) can inform clustering algorithms. We leave this for future work.

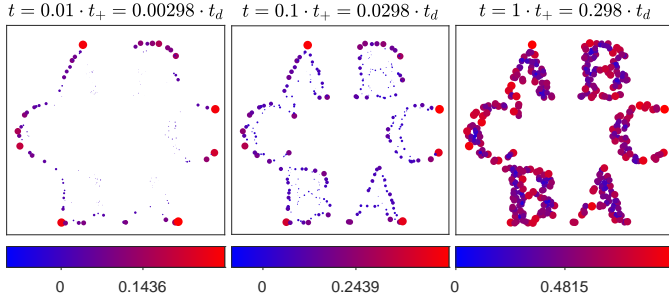


Fig. 2. Weighting components for 500 points sampled without replacement from a probability distribution on \mathbb{Z}^2 that is approximately uniform on its support. From left to right, various scale factors t defining a similarity matrix via $Z = \exp[-td]$ are shown in terms of the intrinsic scales t_d and t_+ (for which see §III). Here d is given by the usual Euclidean distance. Both the color and size of a point are functions of the weighting component; the nonzero color axis tick mark is at half the maximum value.

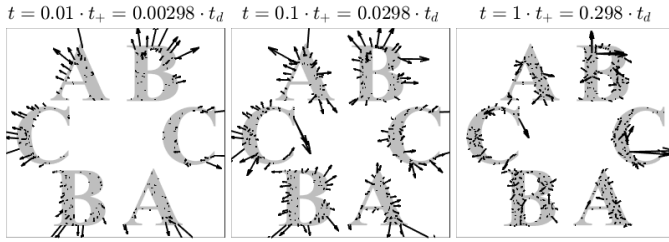


Fig. 3. Weighting gradient estimate (3) for the data in Figure 2. The gradient vectors are scaled uniformly in each panel for visualization purposes. Note that for the largest value of t the large gradient vectors have basepoints near other large gradient vectors.

Thus the sign of $\langle (\hat{\nabla} w)_1, e_1 \rangle$ is the same as that of $\delta - 1$, and the sign of $\langle (\hat{\nabla} w)_2, e_{21} \rangle$ is the opposite. If $\delta = 1$, the flow is stationary. Meanwhile, $\langle (\hat{\nabla} w)_2, e_1 \rangle = -\frac{\sqrt{4-\delta^2}}{2} \langle (\hat{\nabla} w)_2, e_{21} \rangle$, so the isocetes triangle both increases its aspect ratio and experiences an overall shift. In other words, the weighting gradient flow wants to flatten and move the isocetes triangle in the direction suggested by its initial aspect ratio, as shown in Figures 4 and 5.

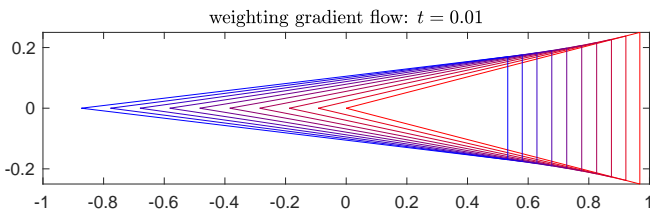


Fig. 4. Effect of weighting gradient flow (4) for Example 3 with $\delta = 0.5 < 1$: evolution goes from red (right) to blue (left). (Note that both axis scales are equal.) Increasing t has the qualitative effect of slowing the flow.

V. ENHANCING DIVERSITY

Following [27], we apply the ideas sketched above to a toy problem where the objective function f has three components, each measuring the distance to a vertex of a regular triangle

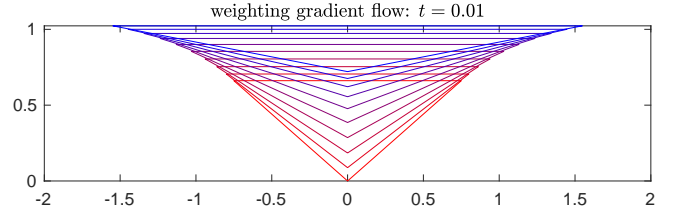


Fig. 5. Effect of weighting gradient flow (4) for Example 3 with $\delta = 1.5 > 1$ (and switching coordinate axes for convenience): evolution goes from red (bottom) to blue (top). (Note that both axis scales are equal.) Increasing t has the qualitative effect of slowing the flow.

with vertices in S^1 . The application is mostly conceptually straightforward, but we mention a few implementation details:

- We begin with a uniformly distributed sample of $n_0 = 10^3$ points in the disk of radius 1.25, and retain n points that are dominated by no more than $\delta = 0.1$;
- Replace any badly behaving points (e.g., out of bounds or NaNs) with their predecessors;¹⁵
- Introduce a “speed factor” $S_j := 1 - 2 \frac{\text{dom}_j}{\max_k \text{dom}_k}$, where dom_j is the number of points dominating the j th point;
- Evolve the n points under a modulated weighting gradient flow on the objective space with $t = t_+$ as $dy_j = ds \cdot S_j (\hat{\nabla} w)_j$ for only $N = 10$ steps and step size $ds = \sqrt{\langle \min_{k \neq j} (d_f)_{jk} \rangle / n}$, where the pullback metric on solution space is $d_f(x, x') := d(f(x), f(x'))$;
- Pull back the weighting gradient flow from the objective space to the solution space using the pseudoinverse of the Jacobian, then recompute points in the objective space.

The result of this experiment is depicted in Figures 6 and 7. The salutary effect on diversity in objective (and solution) space is apparent. This can be quantified via the objective space magnitude functions, as shown in Figures 8 and 9.

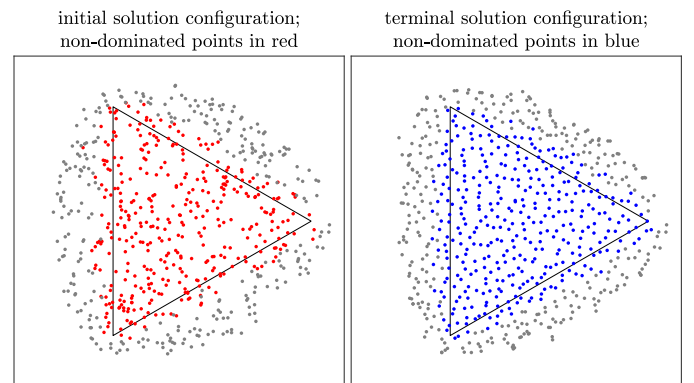


Fig. 6. Comparison of initial (red; left) and terminal (blue; right) locations of points in the solution space. The weighting gradient flow produces more evenly distributed terminal points. The triangle defining objective components (by distance to its vertices) is shown. The actual Pareto front is the interior of the triangle and the area displayed is $[-1, 1]^2$.

¹⁵One notion of “bad behavior” that we do not curtail is of $f(x+dx) - f(x)$ being a poor approximation of dy . The reason is that an effective approximation via Taylor’s theorem requires computing the Hessian, which is expensive. Given an alternative route to an effective approximation, we could instill the required discipline in the pullback/recomputation step below.

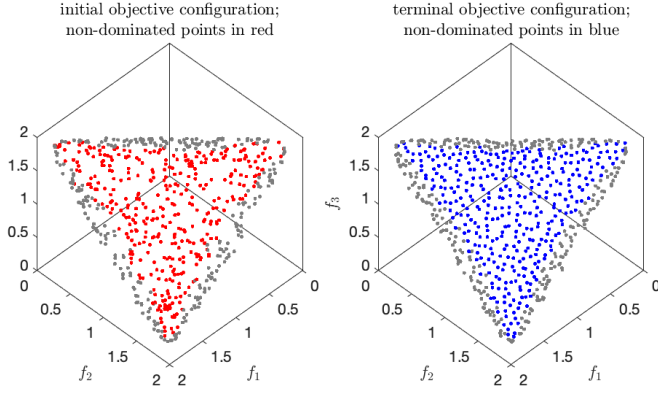


Fig. 7. Comparison of **initial** (red; left) and **terminal** (blue; right) locations of points in the objective space. The terminal points are more evenly distributed.

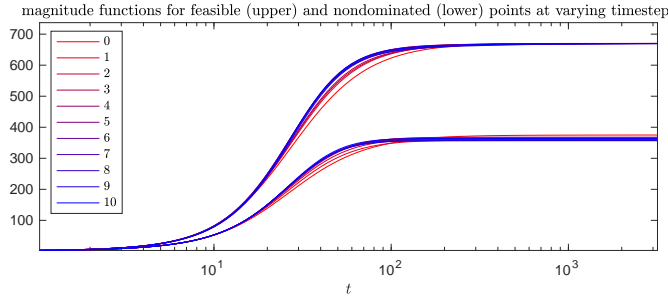


Fig. 8. Magnitude functions (note the logarithmic horizontal axis) for feasible (upper curves) and nondominated points (lower curves) at timesteps (indicated in legend: the horizontal axis corresponds to scale, not time) from 0 (red) to $N = 10$ (blue), under the evolution of the (modulated) weighting gradient flow. Recall from §III that magnitude functions always have left and right limits at 1 and n , respectively, so only intermediate values indicate anything meaningful. Here, the magnitude increases significantly over time at scales $t \approx 50$, while for each timestep $t_+ < 32$. The number of nondominated points fluctuates slightly, starting at 375 before decreasing to 357 and increasing back to 364; there are $n = 670$ feasible points.

Using 12 objectives defined by the distance to vertices of a regular dodecagon but otherwise proceeding in exactly the same way yields the solution space result shown in Figure 10.

VI. PERFORMANCE ON BENCHMARKS

The effectiveness of the (modulated) weighting gradient flow approach hinges on the ability to cover and thereby “keep pressure on” the Pareto front. A straightforward way to do this is to use a MOEA to produce an initial overapproximation of the Pareto front as in [28], and then improve the diversity of the overapproximation via the weighting gradient flow. We proceed to detail the results of an experiment along these lines. For the experiment we considered two leading MOEAs (NSGA-II [29] and SPEA2 [30]) and two leading benchmark

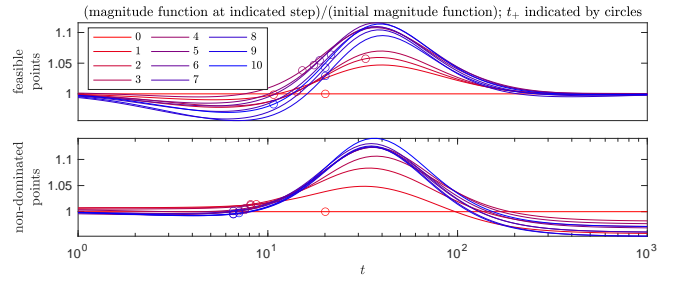


Fig. 9. Magnitude increases at scales above t_+ , where magnitude equals diversity. (Top) Magnitude function quotients (current/initial; cf. Figure 8) at various timesteps for feasible points. Timesteps of numerators are indicated by color, going from **red at the initial timestep** (0) to **blue at the final timestep** ($N = 10$): the denominator is the function at the initial timestep. Circles indicate the scales t_+ . (Bottom) As above, but for non-dominated points.

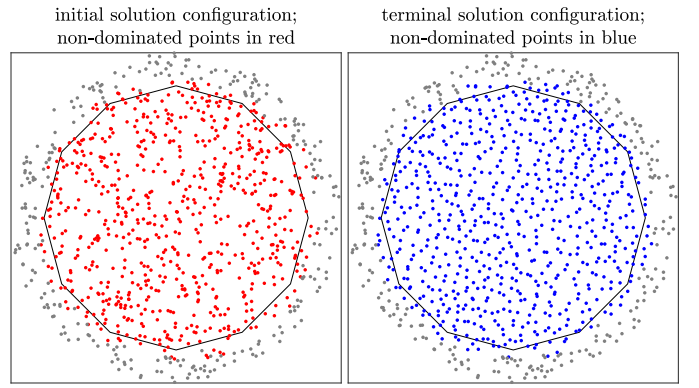


Fig. 10. As in Figure 6 but for a dodecagon.

problem sets (DTLZ [31]¹⁶ and WFG [33]), all implemented in PlatEMO version 2.9 [34]. For each problem, we used 10 decision variables, three objectives (to enable visualization), and performed 10 runs (which appears quite adequate for characterization purposes) with population size 250 and 10^4 fitness evaluations. We then took $N = 10$ timesteps for the weighting gradient flow as before.

Figure 11 (cf. Figure 9) shows magnitude functions corresponding to various timesteps of the (modulated) weighting gradient flow applied to the results of NSGA-II on the benchmark problem WFG2. Feasible points show a diversity (as measured by magnitude at scale t_+ for the feasible objective points) increase of about 10 percent, whereas non-dominated points show a diversity increase of several percent as well, even as the total number of non-dominated points decreases by about 15 percent.

In lieu of showing details such as in Figures 11 for multiple runs and problem instances, we produce an ensemble charac-

¹⁶For DTLZ, we considered only the two most relevant problems, viz. DTLZ4 and DTLZ7. DTLZ4 was formulated “to investigate an MOEA’s ability to maintain a good distribution of solutions” and DTLZ7 was formulated to “test an algorithm’s ability to maintain subpopulation in different Pareto-optimal regions” [31]. (NB. One approach for this, not pursued here, is to resample points so that the diversity per point in each connected component of the Pareto front is approximately equal. For the application of topological data analysis to Pareto fronts, see [32].) The other problems in the DTLZ set are designed to evaluate other desiderata, e.g. convergence to the Pareto front.

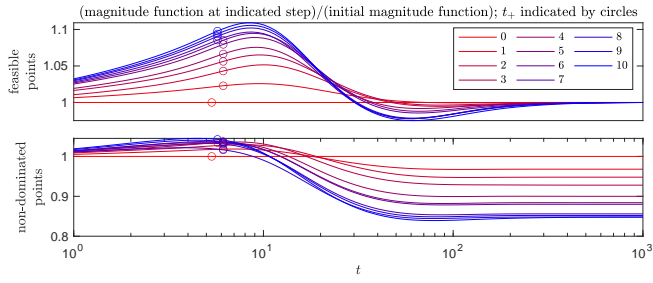


Fig. 11. Magnitude increases at scales above t_+ , where magnitude equals diversity (cf. Figure 9). (Top) Magnitude function quotients at various timesteps for feasible points under the evolution of the (modulated) weighting gradient flow applied to a solution of the WFG2 benchmark problem obtained via NSGA-II. The horizontal axis t indicates the scale parameter; timesteps of numerators are indicated via color, going from red at the initial timestep (0) to blue at the final timestep (10); the denominator is the function at the initial timestep. Circles indicate the scales t_+ . (Bottom) As above, but for non-dominated points. (NB. The corresponding evolution of objective space configurations is shown in Figure 15.)

terization in Figure 12. The figure shows that the number of non-dominated points decreases since the weighting gradient flow pushes some points a short distance away from the Pareto front (as illustrated in Figure 14) before they are halted or reversed. The figure also shows that the diversity of non-dominated points generally increases slightly, and the diversity of feasible points increases significantly. As a consequence, the diversity contributions of individual solutions (as measured by the average weighting, i.e., the magnitude of non-dominated points divided by their cardinality) also increases significantly. For less challenging problems such as shown above for distances to vertices of regular polygons, the number of non-dominated points will decrease less (if at all, cf. Figure 8), and the diversity gains will be enhanced.

On the other hand, the positive effects of the weighting gradient flow are considerably reduced in the case of SPEA2, which produces a visibly more uniform¹⁷ distribution in objective space than NSGA-II for all of the problems we consider: see Figures 17-18. Indeed, the weighting gradient flow appears to *decrease* this uniformity; the formation of a gap just behind the boundary along with a slight increase in the population near the boundary are the main visible indicators that something useful (at least for DTLZ4, WFG2, WFG3, WFG6, and WFG8, per Figure 12) is actually happening.

Although Figure 12 shows that the weighting gradient flow causes a significant proportion of points to become dominated by others, Figure 14 uses the *inverted generational distance* (IGD) relative to uniformly distributed reference points on Pareto fronts [35] to show that this qualitative change in dominance is belied by only minor quantitative changes in the distance to Pareto fronts.¹⁸ (Note that the relatively large increases in IGD for DTLZ4 and DTLZ7 are consequences of starting from a low baseline.) That is, feasible points give a better quantitative picture of diversification performance than

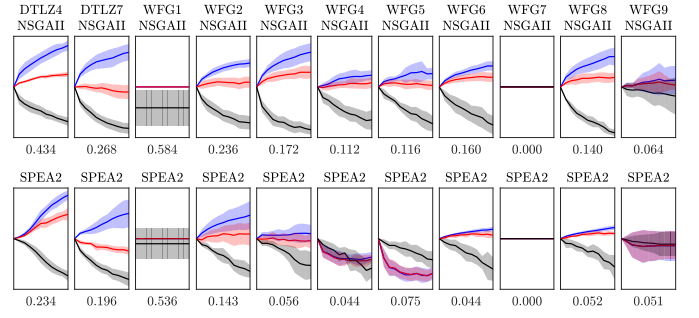


Fig. 12. Diversity of solutions increases markedly under the weighting gradient flow, even as some points become slightly dominated. (Top) Average diversity quotients of *feasible* (blue) and *non-dominated* (red) points under the weighting gradient flow along with proportion of population that remains non-dominated (black). Here the diversity is the magnitude at scale t_+ : for instance, the diversity quotients of feasible and non-dominated points for a particular run of NSGA-II on WFG2 are respectively indicated by the circles in upper and lower panels of Figure 11. Shaded bands indicate one standard deviation. All panels have the same horizontal axis, viz., the number of timesteps (from 0 to $N = 10$). The vertical axes are $[1 - \Delta, 1 + \Delta]$, where Δ is shown below each panel. Not shown explicitly is the average weighting of non-dominated points, i.e., the red curve divided by the black one, but so long as the colored bands already shown are visibly separate, this consistently lies above the blue band. (Bottom) As for the top panels, but for SPEA2.

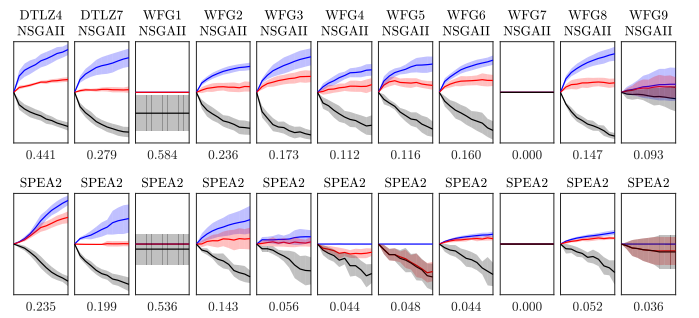


Fig. 13. As in Figure 12, but for diversity taken as the magnitude at the scale maximizing the quotient by the initial timestep.

non-dominated points, especially in light of use cases in which the weighting gradient flow is not limited to postprocessing.

Rather than relying solely on a delicate characterization of diversity, we also visualize some of the results directly: this is the rationale for three-objective problems. Indeed, Figures 15-16 show how diversity in objective space is promoted for WFG2-3. Figures 17-18 show analogous results for SPEA2.

Careful inspection reveals that the weighting gradient flow tends to induce a gap between the boundary of the non-dominated region and its interior, which is consistent with the generally observed phenomenon that the largest weights in finite subsets of Euclidean space tend to occur on boundaries and the smallest weights immediately “behind” the boundary. Meanwhile, the boundary region tends to become slightly more populated.¹⁹ From the perspective of a MOEA, this is frequently a benefit, since extremal and non-extremal points on the non-dominated approximation of the Pareto front fre-

¹⁹This highlights the need to distinguish between diversity and uniformity. In fact, the maximally diverse probability distribution on the interval $[0, L]$ is $\frac{1}{2+L}(\delta_0 + \lambda|_{[0,L]} + \delta_L)$, where Dirac measures and a restriction of Lebesgue measure are indicated on the right hand side [36]. Thus it is only in a suitable limit that boundary effects can be ignored in considerations of diversity.

¹⁷As a reminder, uniformity and diversity are not the same thing.

¹⁸Recall that the IGD of an objective point set X relative to a reference point set R is $\frac{1}{|R|} \sum_{r \in R} \min_{x \in X} d(x, r)$.

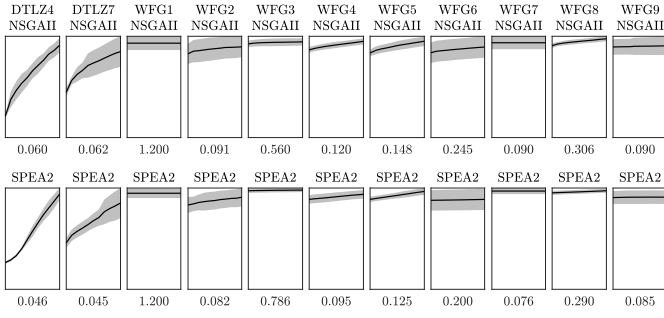


Fig. 14. The weighting gradient flow only slightly affects the quantitative dominance behavior of points, as measured by IGD. (Top) IGD under the weighting gradient flow starting from the results of NSGA-II runs, using uniformly distributed reference points on Pareto fronts. Shaded bands indicate one standard deviation. All panels have the same horizontal axis, viz., the number of timesteps (from 0 to $N = 10$). The vertical axes are $[0, y]$, where y is shown below each panel. (Bottom) As for the top panels, but for SPEA2.

quently carry different practical significance.²⁰

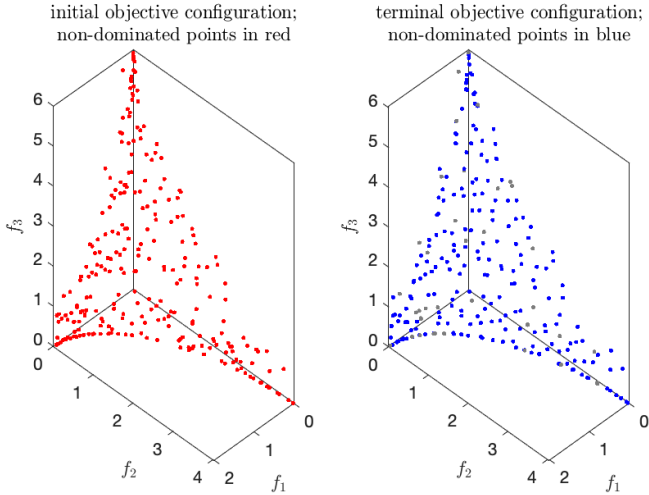


Fig. 15. (Left) Initial configuration in objective space for WFG2 after a NSGA-II run. (Right) Terminal configuration for WFG2 after subsequently evolving under the weighting gradient flow. Dominated points are gray.

VII. ALGORITHMIC EXTENSIONS

A. Multi-objective weighting gradient flow

We can combine the weighting gradient flow with a multi-gradient descent strategy in a way somewhat akin to [37]. The basic ideas that build on the weighting gradient flow are:

- Introduce variable regularizing terms λ_w and λ_f for the weighting and function gradient flows, respectively;
- Form the objective-space differentials $dy_j = ds \cdot [\lambda_w S_j(\hat{\nabla} w)_j + \lambda_f \sum_{\ell} (\hat{\nabla} f)_{\ell}]$, where the sum is over ℓ such that $\langle (\hat{\nabla} w)_j, (\hat{\nabla} f)_{\ell} \rangle > 0$.

While we have tried this technique in isolation on MOEA benchmark problems, the results are poor. However, this

²⁰Using a scale $t > t_+$ for the weighting gradient flow would tend to diminish the distinction between uniformity (which is not a function of scale) and diversity (which is a function of scale). In other words, our experiments deliberately magnify this distinction to the greatest possible extent.

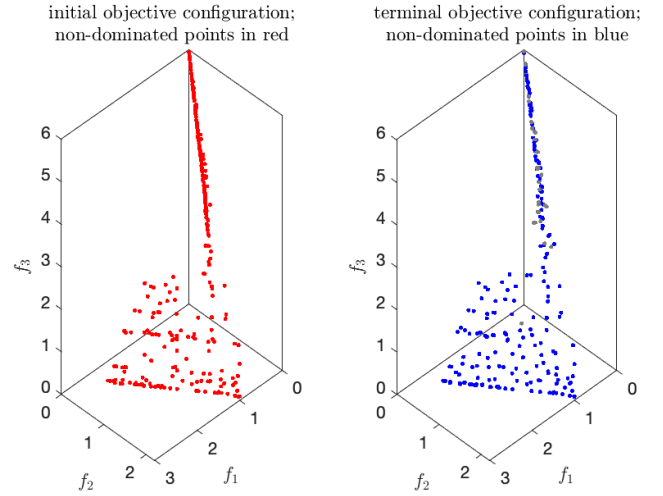


Fig. 16. As in Figure 15, but for WFG3.

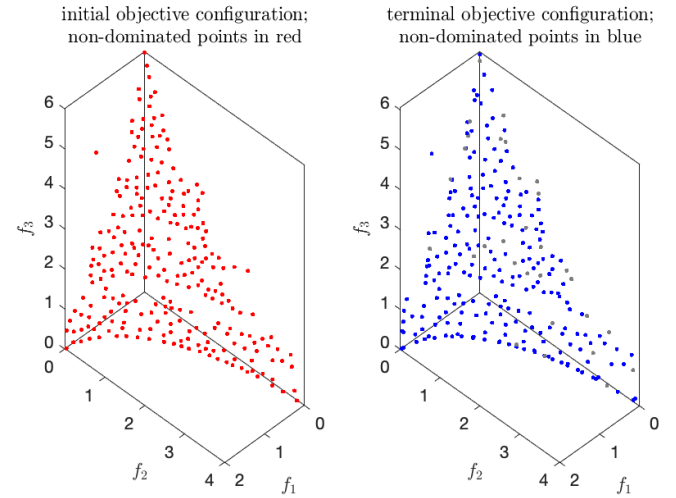


Fig. 17. As in Figure 15, but for SPEA2.

should come as no surprise: the benchmark problems are designed to frustrate MOEAs, to say nothing of techniques involving gradients.

B. Recycling function evaluations

In our experiments with post-processing the output of MOEAs, the weighting gradient flow evolution took time comparable to (and in the case of NSGA-II, slightly more than) the MOEA itself. Most of the time is spent evaluating the fitness function: apart from an initialization step, the evaluations are performed to compute Jacobians in service of pullback operations, and a lesser number are performed to compute pushforwards to maintain consistency.

However, our motivating problems require significant time (on the order of a second) for function evaluations. This demands a more efficient pullback scheme that minimizes (or avoids altogether) function evaluations, even if the results are substantially worse. A reasonable idea is “recycling” in a sense similar to that employed in some modern Monte Carlo

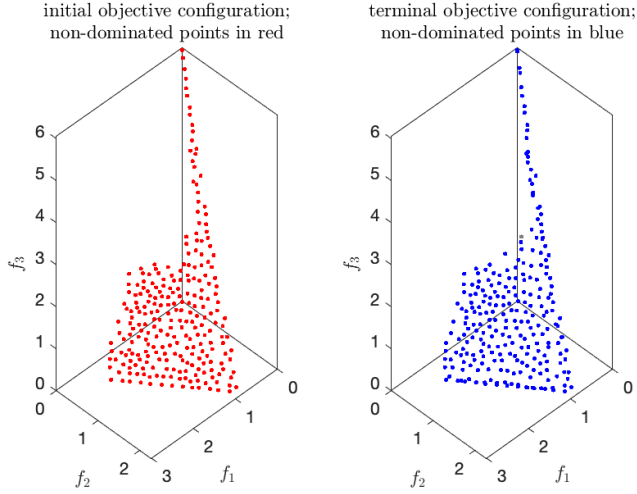


Fig. 18. As in Figure 16, but for SPEA2.

algorithms [38]. Specifically, rather than computing a good approximation to the Jacobian by evaluating functions afresh at very close points along coordinate axes, settle instead for an approximation of lesser quality that exploits existing function evaluations. We have implemented this approach in concert with a *de novo* computation of the Jacobian in the event that this initial Jacobian estimate (IJE) does not have full rank. Our experiments suggest that this approach works reasonably well: for a typical run from §VI, the number of function evaluations is reduced from 30250 to 2750, and the actual results are broadly comparable (sometimes better, sometimes worse): see Figures 19 and 20.

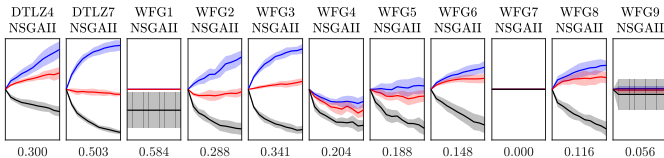


Fig. 19. As in the top panel of Figure 12, but for a Jacobian approximation that uses existing function evaluations, increasing speed at the cost of accuracy.

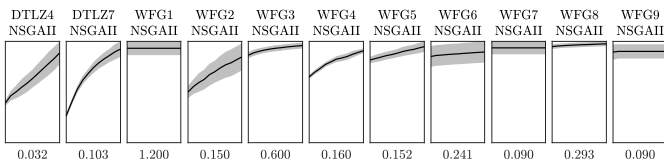


Fig. 20. As in Figure 14, but for a Jacobian approximation that uses existing function evaluations, increasing speed at the cost of accuracy.

This strategy is bound to work poorly if our evaluation points lie on a manifold of nonzero codimension or low curvature, because in such circumstances a matrix that transforms vectors from a base point to evaluation points into (a small multiple of) the standard basis will have large condition

number.²¹ However, these situations are relatively unlikely to present major problems in practice, and the recycling approach is likely to be useful in most if not all situations where function evaluations are expensive.

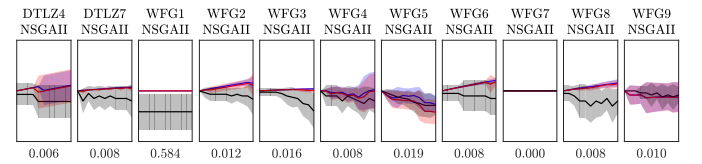
C. Using spread instead of magnitude

A more principled approximation of the magnitude than [4], [5] use is the *spread* [39]. In some respects, the spread is even better behaved than the magnitude and requires only $O(n^2)$ operations with a naive algorithm. The idea is to take the *Leinster-Cobbold diversity* [40] of order zero for the uniform distribution, i.e.

$$E_0(d) := \sum_j \frac{1}{\sum_k \exp(-d_{jk})}. \quad (5)$$

It turns out that $E_0(d)$ is bounded above by the maximum diversity of d (which itself is bounded above by magnitude if d is positive definite) and also by $\exp \max_{jk} d_{jk}$. Furthermore, $E_0(td)$ increases from 1 at $t = -\infty$ to n at $t = \infty$. Finally, $E_0(d)$ itself admits a good approximation by truncating the sums involved, and with some care this can reduce the computational effort compared to the naive algorithm.

If we define $a_j := 1/\sum_k \exp(-d_{jk})$, then $E_0(d) = \sum_j a_j$, and we can consider the gradient flow obtained by using the “spread vector” a in place of a weighting. However, this does not yield useful results, as shown in Figure 21.

Fig. 21. As in the top panel of Figure 12, but for a gradient flow using the “spread vector” a in lieu of a weighting at scale t_+ . Not shown: dilating d by t_+ does not have any substantial effect.

D. Other considerations

At present, we have not explored stochastic gradient descent and/or line search techniques to improve performance: however, it seems likely that these would be at best delicate to implement successfully. While we could restrict the summations involved in the weighting gradient flow, these have a comparatively small impact on runtime. Other avenues for

²¹A more refined approach would be to exploit the “good” points, evaluating the function afresh in new directions in order to get reasonably well-behaved Jacobian estimates. A rough sketch of this approach is to compute a SVD of the IJE, then use this in turn to estimate the rank. If the rank is not full, then revise the IJE as follows. First, the pivots for the reduced row echelon form of the IJE yield a maximal linearly independent subset of the columns. To augment these columns, reuse the SVD to produce their orthocomplement (which equals the kernel of the transpose of the IJE, which itself is determined by the transpose of the rows of the first term in the SVD that correspond to zero singular values). After performing any necessary function evaluations in the orthocomplement, finally apply a linear transformation that yields a revised Jacobian estimate in the standard basis. This more refined approach is sufficiently intricate that we have not implemented it.

acceleration appear to be restricted to computing or approximating weightings more efficiently. There is much that can be done in this vein, but we omit discussion for economy.

It seems fruitful to consider non-differentiable variants of the weighting gradient flow (for this, see §VIII). With this in mind, we recall an abstract perspective on genetic algorithms provided by [41], which points out in turn that a sequential Monte Carlo (SMC; e.g., a particle filter) algorithm is essentially a Markov chain Monte Carlo (MCMC) algorithm operating over a population versus an individual, and that a genetic algorithm is essentially a SMC algorithm that makes use of genetic-type operations.²² Now a MOEA is essentially a genetic algorithm that addresses multiple objectives.

From this perspective, and abstracting some of the techniques we have developed, we can envision the broad outlines of a MOEA that leverages weightings in a principled and coherent set of internal mechanisms with the aim of outperforming existing algorithms:

- Population: use an existing SMC algorithm or extend a fast multiple-proposal MCMC technique such as [42] to accept multiple proposals and maintain a population;
- Genetic-type operations: intersperse general-purpose (and possibly also domain-specific) genetic-type operations with a mechanism for favoring increases to individual weighting components (e.g., eliminate points with small absolute values of weighting components and replenish the population with “spores” distributed around points with large weighting components);
- Multiple objectives: compare state-space moves that increase weighting components with those that favor objectives, and select moves that accomplish both, with regularization terms to make an explore (weighting)-exploit (objective) tradeoff.

VIII. DISCRETE OBJECTIVE SPACE

Suppose that $f : X \rightarrow Y \subset \mathbb{R}^m$ for Y countable and that \mathbb{R}^m is endowed with a suitable distance d which need not be a metric, let alone Euclidean. Now the weighting gradient (3) still makes sense on Y , though the weighting gradient flow (4) does not make sense any more. However, for $x \in X$ and δx a suitable random perturbation, comparing $f(x + \delta x)$ and $f(x) + \delta s \cdot \hat{\nabla} w|_{f(x)}$ over multiple realizations of δx yields a stochastic analogue of (the pullback of) (4):

$$\hat{\delta} x|_x := \arg \min_{\delta x} d \left(f(x + \delta x), f(x) + \delta s \cdot \hat{\nabla} w|_{f(x)} \right). \quad (6)$$

A sensible heuristic for δs in (6) is to enforce something like $\langle |\delta s \cdot \hat{\nabla} w| \rangle = \delta d/2$ initially, where δd is the average Euclidean distance between pairs of initial points in Y with minimal nonzero d . That is, take $\delta s = \delta d/2 \langle |\hat{\nabla} w| \rangle$. This would

seem to encourage the movement of significant numbers of points while a significant fraction of points would also remain stationary for the first timestep. Meanwhile, a reasonable heuristic for δx in the case $X \subset \mathbb{R}^M$ is to take $\delta x \sim \mathcal{N}(\mu, \Sigma)$, where $\mu = D_x f \setminus (\hat{\nabla} w|_{f(x)})$, $\Sigma = \Delta(|\mu|, \delta_j, \dots, \delta_j)$ in an(y) orthonormal basis with first vector μ ,²³ and where $\delta_j := \frac{1}{2} \min_{k \neq j} |x_j - x_k|$.

Note that while (6) can be approximated using a meta-heuristic, the spirit of applications is to take a relatively small number of candidate perturbations δx versus finding the optimal perturbation *per se*. With this in mind, define the *effort* $E(x)$ to be the number of candidate perturbations for x . If we can neglect any effects of perturbing the same points over successive timesteps, a sensible heuristic for effort is

$$E(x) = \left\lceil C \frac{|\hat{\nabla} w|_{f(x)}}{\sum_{x'} |\hat{\nabla} w|_{f(x')}} \right\rceil \quad (7)$$

for a constant C that approximately determines the overall effort. This heuristic simply distributes effort to each point according to its “need” to be perturbed as measured by its weighting gradient.

If points occupy the same positions for a long time (say, because the geometry of f inhibits their movement), another sensible heuristic attuned to this behavior is an effort defined in terms of the effective energies of points *à la* [43], using the cumulative occupation times of positions to define probabilities and some notion of (e.g.) convergence rate (which in general will vary over time) to define the overall timescale required for the framework. This heuristic will focus effort on positions that have been occupied the least amount of time while encouraging all positions to be uniformly occupied.

Shifting gears, consider the situation where we have no objective f and X is completely generic, so that even the weighting gradient is not necessarily defined. Suppose we have $\{x_j\}_{j=1}^n \subset X$ and distance matrix $d_{jk} = d(x_j, x_k)$. Let w be the weighting at t_+ and select an index j_* with small weighting component w_{j_*} . Now sample x' from a “proposal” distribution $\mathbb{P}(x'|x_{j_*})$ and compare the magnitudes $\mu := \text{Mag}(t_+; \{x_j\}_{j=1}^n)$ and $\mu' := \text{Mag}(t_+; \{x_j\}_{j \neq j_*} \cup \{x'\})$, where we use the same (original) value of t_+ in both instances. If $\mu' \geq \mu$ then replace x_{j_*} with x' ; also, if $\mu' < \mu$ and $x' \notin \{x_j\}_{j \neq j_*}$, do the same thing with probability $\exp(-\beta[\mu - \mu'])$ for some suitable $\beta < 0$. That is, perform a Metropolis-Hastings step according to the proposal.²⁴ This sort of technique works in great generality, and its efficiency is determined largely by that the the proposal.

IX. REMARKS

Although our experiments have focused on the results of applying the weighting gradient flow and related constructions after a MOEA has been applied, the more natural application is in the course of a MOEA. As mentioned in §VII and VIII,

²²Nominally, these are usually thought of as, e.g. mutation, crossover, and selection. But at a more abstract level, a genetic algorithm sampling from a Markov random field has an objective in which all of the terms involve local interactions between variables. A reasonable genetic-type operation must respect the topology of these interactions, as encoded in a factor graph (or equivalently, the abstract simplicial complex encoding the relation between factors and variables). In other words, the operation must involve a reasonable mechanism for segmentation, i.e., partitioning variables and manipulating them in a way that is compatible with the partition.

²³To produce a matrix B whose columns form an orthonormal basis with first vector a in MATLAB, use `ahat = a(:) ./ norm(a); B = [ahat; null(ahat)']'`.

²⁴More generally, we can make multiple proposals for x' and use one of the acceptance mechanisms described in [42].

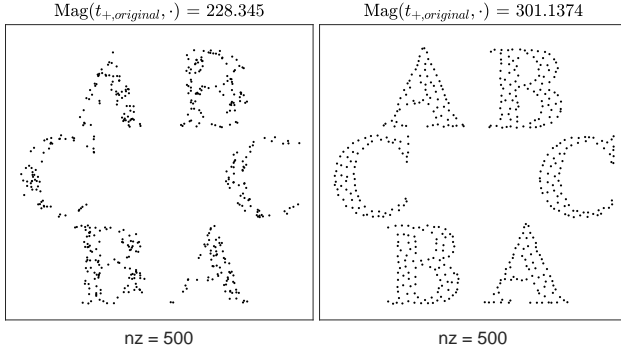


Fig. 22. (Left) 500 points sampled as in Figure 2. (Right) The result of the following process: for each of 1000 timesteps, we select the 10 points with least weighting component (at the original value of t_+) and sample 10 corresponding candidate points outside of the current locations and without replacement; then (and in ascending order of weighting component) test to see if the overall magnitude increases upon substituting the candidate point (i.e., perform a Metropolis-Hastings step for $\beta = \infty$). The magnitude increases by almost 32 percent.

there is ample scope to refine and build on ideas for increasing weighting components in specific contexts. It is nevertheless clear that the theory of magnitude informs principled and practical diversity-promoting mechanisms that can already be usefully applied to benchmark multi-objective problems.

APPENDIX A EROSION

In the setting of Euclidean space we can iteratively down-sample a finite set B to obtain $B' \subseteq B$ with positive weights. The idea is as follows. Let $Z_{jk} := \exp(-d(b_j, b_k))$ and let w be the unique weighting for Z .²⁵ Now set $B' = B$, $w' = w$, and repeatedly reassign $B' \leftarrow \{b_j \in B' : w'_j > 0\}$ and recompute Z' and w' until the corresponding weighting is positive. This iteration terminates in a unique $B' \neq \emptyset$ admitting a positive weighting. When normalized, this weighting maximizes diversity on B' , as depicted in Figure 23.

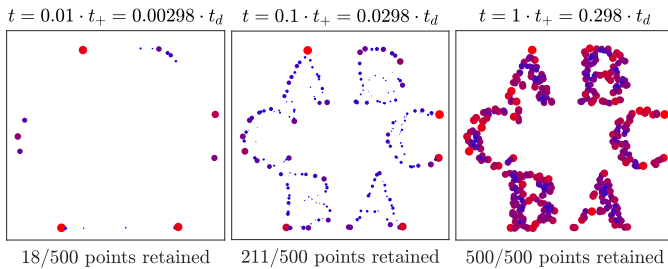


Fig. 23. From left to right: diversity-saturating weightings on erosions of the set from Figure 2 for varying scale factors t . The number of points retained in each erosion is shown. Both the color and size of a point is a function of the weighting component.

In short, we can enforce the existence of a positive weighting by scaling or eroding, depending on whether the scale

²⁵In an arbitrary metric space, we may not have a weighting at all, let alone a unique one. However, the absence or nonuniqueness of any weighting is a degenerate pathology that can be avoided by perturbations.

or elements of the data should be prioritized. Provided we ignore (points with) lesser weights, the two approaches appear to yield qualitatively similar results.

ACKNOWLEDGMENT

Thanks to Andy Copeland, Megan Fuller, Zac Hoffman, Rachelle Horwitz-Martin, and Daryl St. Laurent for many patient questions and observations that clarified and simplified the ideas herein. This research was developed with funding from the Defense Advanced Research Projects Agency (DARPA). The views, opinions and/or findings expressed are those of the author and should not be interpreted as representing the official views or policies of the Department of Defense or the U.S. Government. DISTRIBUTION STATEMENT A. Approved for public release; distribution is unlimited.

REFERENCES

- [1] A. E. Eiben and J. E. Smith, *Introduction to Evolutionary Computing*. Springer, 2015.
- [2] V. Basto-Fernandes, I. Yevseyeva, A. Deutz, and M. Emmerich, “A survey of diversity oriented optimization: problems, indicators, and algorithms,” in *EVOLVE—A Bridge between Probability, Set Oriented Numerics and Evolutionary Computation VII*. Springer, 2017, pp. 3–23.
- [3] J. Yan, C. Li, Z. Wang, L. Deng, and D. Sun, “Diversity metrics in multi-objective optimization: review and perspective,” in *2007 IEEE International Conference on Integration Technology*. IEEE, 2007, pp. 553–557.
- [4] T. Ulrich, J. Bader, and L. Thiele, “Defining and optimizing indicator-based diversity measures in multiobjective search,” in *International Conference on Parallel Problem Solving from Nature*. Springer, 2010, pp. 707–717.
- [5] T. Ulrich and L. Thiele, “Maximizing population diversity in single-objective optimization,” in *Proceedings of the 13th Annual Conference on Genetic and Evolutionary Computation*, 2011, pp. 641–648.
- [6] A. R. Solow and S. Polasky, “Measuring biological diversity,” *Environmental and Ecological Statistics*, vol. 1, no. 2, pp. 95–103, 1994.
- [7] T. Leinster, *Entropy and Diversity: the Axiomatic Approach*. Cambridge, 2021.
- [8] E. Zitzler and S. Künzli, “Indicator-based selection in multiobjective search,” in *International Conference on Parallel Problem Solving from Nature*. Springer, 2004, pp. 832–842.
- [9] Y. Wang, M. Emmerich, A. Deutz, and T. Bäck, “Diversity-indicator based multi-objective evolutionary algorithm: Di-moea,” in *International Conference on Evolutionary Multi-Criterion Optimization*. Springer, 2019, pp. 346–358.
- [10] J. K. Pugh, L. B. Soros, and K. O. Stanley, “Quality diversity: A new frontier for evolutionary computation,” *Frontiers in Robotics and AI*, vol. 3, p. 40, 2016.
- [11] M. D. Buhmann, *Radial basis functions: theory and implementations*. Cambridge, 2003, vol. 12.
- [12] B. Schölkopf, R. Herbrich, and A. J. Smola, “A generalized representer theorem,” in *International conference on computational learning theory*. Springer, 2001, pp. 416–426.
- [13] I. Steinwart and A. Christmann, *Support vector machines*. Springer, 2008.
- [14] S. Willerton, “Heuristic and computer calculations for the magnitude of metric spaces,” *arXiv preprint arXiv:0910.5500*, 2009.
- [15] E. Bunch, D. Dickinson, J. Kline, and G. Fung, “Practical applications of metric space magnitude and weighting vectors,” *arXiv preprint arXiv:2006.14063*, 2020.
- [16] M. W. Meckes, “Magnitude, diversity, capacities, and dimensions of metric spaces,” *Potential Analysis*, vol. 42, no. 2, pp. 549–572, 2015.
- [17] S. R. S. Varadhan, “On the behavior of the fundamental solution of the heat equation with variable coefficients,” *Communications on Pure and Applied Mathematics*, vol. 20, no. 2, pp. 431–455, 1967.
- [18] G. Peyré, M. Cuturi *et al.*, “Computational optimal transport: with applications to data science,” *Foundations and Trends® in Machine Learning*, vol. 11, no. 5-6, pp. 355–607, 2019.

- [19] T. Leinster and M. W. Meckes, “The magnitude of a metric space: from category theory to geometric measure theory,” in *Measure Theory in Non-Smooth Spaces*, N. Gigli, Ed.
- [20] —, “Maximizing diversity in biology and beyond,” *Entropy*, vol. 18, no. 3, p. 88, 2016.
- [21] M. W. Meckes, “Positive definite metric spaces,” *Positivity*, vol. 17, no. 3, pp. 733–757, 2013.
- [22] R. Rammal, G. Toulouse, and M. A. Virasoro, “Ultrametricity for physicists,” *Reviews of Modern Physics*, vol. 58, no. 3, p. 765, 1986.
- [23] T. Leinster, “The magnitude of metric spaces,” *Documenta Mathematica*, vol. 18, pp. 857–905, 2013.
- [24] R. A. Horn and C. R. Johnson, *Matrix Analysis*. Cambridge, 2012.
- [25] C. Luo, I. Safa, and Y. Wang, “Approximating gradients for meshes and point clouds via diffusion metric,” in *Computer Graphics Forum*, vol. 28, no. 5. Wiley Online Library, 2009, pp. 1497–1508.
- [26] B. Andrews, B. Chow, C. Guenther, and M. Langford, *Extrinsic Geometric Flows*. AMS, 2020.
- [27] H. Ishibuchi, M. Yamane, N. Akedo, and Y. Nojima, “Two-objective solution set optimization to maximize hypervolume and decision space diversity in multiobjective optimization,” in *The 6th International Conference on Soft Computing and Intelligent Systems, and The 13th International Symposium on Advanced Intelligence Systems*. IEEE, 2012, pp. 1871–1876.
- [28] G. Guariso and M. Sangiorgio, “Improving the performance of multi-objective genetic algorithms: An elitism-based approach,” *Information*, vol. 11, no. 12, p. 587, 2020.
- [29] K. Deb, A. Pratap, S. Agarwal, and T. Meyarivan, “A fast and elitist multiobjective genetic algorithm: Nsga-ii,” *IEEE transactions on evolutionary computation*, vol. 6, no. 2, pp. 182–197, 2002.
- [30] E. Zitzler, M. Laumanns, and L. Thiele, “Spea2: Improving the strength pareto evolutionary algorithm,” *TIK-report*, vol. 103, 2001.
- [31] K. Deb, L. Thiele, M. Laumanns, and E. Zitzler, “Scalable test problems for evolutionary multi-objective optimization,” *TIK-Report*, vol. 112, 2001.
- [32] N. Hamada and K. Goto, “Data-driven analysis of pareto set topology,” in *Proceedings of the Genetic and Evolutionary Computation Conference*, 2018, pp. 657–664.
- [33] S. Huband, P. Hingston, L. Barone, and L. While, “A review of multiobjective test problems and a scalable test problem toolkit,” *IEEE Transactions on Evolutionary Computation*, vol. 10, no. 5, pp. 477–506, 2006.
- [34] Y. Tian, R. Cheng, X. Zhang, and Y. Jin, “Platemo: A matlab platform for evolutionary multi-objective optimization [educational forum],” *IEEE Computational Intelligence Magazine*, vol. 12, no. 4, pp. 73–87, 2017.
- [35] Y. Tian, X. Xiang, X. Zhang, R. Cheng, and Y. Jin, “Sampling reference points on the pareto fronts of benchmark multi-objective optimization problems,” in *2018 IEEE congress on evolutionary computation (CEC)*. IEEE, 2018, pp. 1–6.
- [36] T. Leinster and E. Roff, “The maximum entropy of a metric space,” *arXiv preprint arXiv:1908.11184*, 2019.
- [37] J.-A. Désidéri, “Multiple-gradient descent algorithm (mgda) for multi-objective optimization,” *Comptes Rendus Mathématique*, vol. 350, no. 5-6, pp. 313–318, 2012.
- [38] D. Frenkel, “Speed-up of monte carlo simulations by sampling of rejected states,” *Proceedings of the National Academy of Sciences*, vol. 101, no. 51, pp. 17 571–17 575, 2004.
- [39] S. Willerton, “Spread: a measure of the size of metric spaces,” *International Journal of Computational Geometry & Applications*, vol. 25, no. 03, pp. 207–225, 2015.
- [40] T. Leinster and C. A. Cobbold, “Measuring diversity: the importance of species similarity,” *Ecology*, vol. 93, no. 3, pp. 477–489, 2012.
- [41] D. Mumford and A. Desolneux, *Pattern theory: the stochastic analysis of real-world signals*. CRC Press, 2010.
- [42] S. Huntsman, “Fast markov chain monte carlo algorithms via lie groups,” in *International Conference on Artificial Intelligence and Statistics*, 2020, pp. 2841–2851.
- [43] —, “Sampling and statistical physics via symmetry,” in *Joint Structures and Common Foundation of Statistical Physics, Information Geometry and Inference for Learning*, F. Barbaresco and F. Nielsen, Eds. Springer, 2021.